Performance of AMB Suspended Energy Storage Flywheel Controllers in the Presence of Time Delays

Xujun Lyu[a,b], Long Di[c], Zongli Lin[d], Yefa Hu[b], Huachun Wu[b]

[a] College of Engineering, Huazhong Agricultural University, Wuhan, Hubei 430070, China. Email:lyuxujun@mail.hzau.edu.cn
[b] School of Mechanical and Electronic Engineering, Wuhan University of Technology, Wuhan, Hubei 430070, China. Email: {lyuxujun, huyefa, whc}@whut.edu.cn
[c] ASML-HMI, 1762 Automation Pkwy, San Jose, CA 95131, USA. Email: ld4vv@virginia.edu
[d] Charles L. Brown Department of Electrical and Computer Engineering, University of Virginia, Charlottesville, VA 22904-4743, USA. Email: zl5y@virginia.edu

***Abstract*—A flywheel suspended on active magnetic bearings (AMBs) constitutes a complex system including a rotor, flywheel disks, active magnetic bearings, auxiliary bearings, a motor/generator, control systems and energy conversion systems. The complexity of AMB suspended flywheel systems often makes the construction of their test rigs too costly in a research laboratory. We recently developed an experimental platform for AMB suspended energy storage flywheel. This platform serves as a test rig to assist the analysis and control design and was developed on the basis of a flexible rotor-AMB test rig previously constructed in the Rotating Machinery and Controls (ROMAC) Laboratory, University of Virginia. Two different control designs have been implemented on this platform: the μ-synthesis control and the characteristic model based all coefficient adaptive control (ACAC). In this paper, we examine the performance of the test rig in the presence of time delays. In particular, we show by simulation that this control design possesses considerable ability to resist the effect of time delays in the control inputs and/or output measurements.**

I. Introduction

In recent years, with the development of renewable energy generation technology, the proportion of renewable energy contributing to the power grid, such as wind power generation, solar photovoltaic power generation and hydraulic power generation, increases rapidly, which brings an urgent demand on the energy storage technology applied in the power grid [7]. The emergence of energy storage technology solves the volatility and intermittent problems of renewable energy generation flowing into the power grid, and becomes one of the key technology to ensure the safe, stable and economic operation of the power grid [2]. Flywheel energy storage systems, a typical mechanical energy storage technology, with appealing features such as high power density, high energy efficiency, short recharge times, wide operating temperature ranges and long life cycles ([3], [4]), have found applications in pulse power supplies for linear induction launchers, energy storage devices for grid frequency regulation, power leveling, voltage sag mitigation, uninterruptible power supplies, and hybrid configuration with other types of energy storage devices, and have also been used as gyroscopes for simultaneous attitude control and energy storage in space applications ([5], [6]). During the charging process, the kinetic energy is stored in a high-speed rotating disk and is released to the load in the discharging time [7]. Active magnetic bearings (AMBs), with their appealing features of no friction, no wear, no lubrication, low losses, fast response, adjustable support magnetic forces and long lifetime [8], make high speed operation of flywheels possible and are thus the ideal support for high-speed flywheel rotors. The AMBs however require control systems, which have turned out to be quite sophisticated for energy storage flywheels [9].

A flywheel AMB system consists of a rotor, flywheel disks, active magnetic bearings, auxiliary bearings, a motor/generator, control systems and an energy conversion system. The complexity of AMB suspended flywheel systems often makes the construction of their test rigs too costly in a research laboratory. The absence of past operational data makes the implementation of flywheel AMB system feedback control designs more difficult [10]. For these reasons, we recently developed an experimental platform for AMB suspended energy storage flywheel. This platform was aimed to assist the analysis and control design and was developed on the basis of a flexible rotor-AMB test rig previously constructed in the Rotating Machinery and Controls (ROMAC) Laboratory, University of Virginia [11]. By utilizing the two additional AMBs on the test rig, the platform emulates an equivalent rotordynamic characteristics of an energy storage flywheel, and thus serves as a realistic AMB suspended energy storage flywheel test rig to study the feedback control design on.

Feedback control of active magnetic bearing (AMB) suspended energy storage flywheel systems is critical in the operation of the systems and has been well studied. Both the classical proportional-integral-derivative (PID) control design method [12]–[14] and modern control theory, such as H_∞ control [15] and μ-synthesis [16], have been explored. PID control is easy to implement but is not effective in handling complex rotordynamics. Modern control design methods usually require a plant model and an accurate characterization of the uncertainties. Di et al. [17] explored the application of characteristic model based all coefficient adaptive control

(ACAC), originally proposed by Wu ([18], [19]), to a flexible rotor-AMB system, which resulted in lower levels of vibration compared with a benchmark μ-synthesis controller. We implemented the characteristic model based ACAC on the platform mentioned above in [20]. Despite its simplicity, the characteristic model based ACAC was shown to be capable of achieving strong control performance by both simulation and experimental results [20]. It suppresses the vibration on the AMB suspended flywheel test rig to a significantly higher level than an originally designed μ-synthesis controller could [11].

In a complex electromechanical system, due to the limited speed of signal transmission and information processing, the phenomenon of time delay is inevitable [21]. Particularly, when the electronic components of the flywheel AMB control system are placed at a distance from the actuators, cabling in the control loops. Especially in some applications such as tidal power generation and wind power generation where the flywheel AMB system serves as an energy storage device, the adverse effect of time delay phenomenon is obvious. The existence of time delay on the control input and sensor output often causes the deterioration of the system performance and the instability of the system. In the research field of the AMB system, some works about the AMB control system with time delays can be found. Ren [22] analyzed the effects of time delay on the stability of the rotation modes for the magnetically suspended flywheel with strong gyroscopic effects. Kascak [23] considered a simple time delay model of the flywheel supported on rigid rotor and magnetic bearings using PD controller and described a modeling effort used to understand the stability boundaries of the PD controller. Yoon et al. [24] studied the effect of input delay in the control of AMBs in remote rotating machines and adopted the truncated predictor feedback (TPF) control design to maximize the input delay that the stable closed loop system can tolerate. In this paper, we examine the performance in the presence of time delays of the characteristic model based ACAC on the AMB suspended energy storage flywheel experimental platform we developed in [11].

The remainder of this paper is organized as follows. Section II briefly recalls some results of the AMB suspended flywheel characteristic model based ACAC design we recently developed in [20]. Section III investigates the performance of the characteristic model based ACAC with control input delay, displacement measurement delay and both by simulation. Finally Section IV draws the conclusion to the paper.

II. Review of the AMB Suspended Flywheel Characteristic Model Based ACAC

In [20], we carried out the characteristic model based ACAC on an economical and effective platform [11] that we previously developed as a test rig for flywheel AMB system control designs.

A. The AMB Suspended Flywheel Test Rig

Based on the finite element method, the rotordynamic model of the flywheel AMB system are derived from the motion equation described by

$$M\ddot{q} + (C + \Omega G)\dot{q} + Kq = B_{\mathrm{m}}F_{\mathrm{mag}} + B_{\mathrm{e}}F_{\mathrm{ext}}, \qquad (1)$$

where,

M : the symmetric flywheel rotor mass matrix,
C : the symmetric damping matrix,
G : the skew-symmetric gyroscopic effect matrix,
K : the symmetric stiffness matrix,
Ω : the rotational speed,
B_{m} : the position distribution matrix of the support AMBs
F_{mag} : the forces provided by support AMBs,
B_{e} : the position distribution matrix of the external forces
F_{ext} : the external forces acting on the rotor,
q : the generalized displacement vector.

Compared to a usual rotor-AMB system, two important features of a flywheel rotor suspended on AMBs is the negative stiffness of the generator and the gyroscopic effects caused by the flywheel disk [4]. In [11] we proposed to emulate the operation of an energy storage flywheel on an existing flexible rotor-AMB test rig that was previously constructed and developed an economical and effective platform that serves as a test rig for flywheel control designs. The flexible AMB suspended rotor in ROMAC [16] is shown in Figure 1. Specifically, we use the two support AMBs at the non-driven end (NDE) and the driven end (DE) of the rotor to ensure the stable operation of the system. We use the exciter AMB at the quarter span to emulate the negative stiffness induced by the generator and two exciter AMBs at the mid span and the quarter span from the driven end of the rotor to generate gyroscopic coupling resulting from the flywheel disk as shown in Figure 2.

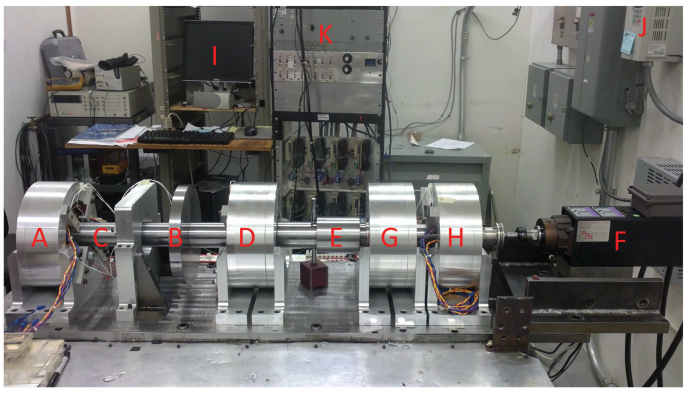

A: Non-driven End Support AMB
B: Gyroscopic Disk 1
C: Rotor Shaft
D: Mid-span Disturbance AMB
E: Gyroscopic Disk 2
F: Electric Motor
G: Quarter-span Disturbance AMB
H: Driven End Support AMB
I: Control Station
J: Variable Frequency Drive
K: Amplifiers & Sensor Conditioning Station

Figure 1: A photograph of the ROMAC flexible rotor-AMB test rig.

Main components of the ROMAC flexible rotor-AMB test rig are described as follows.

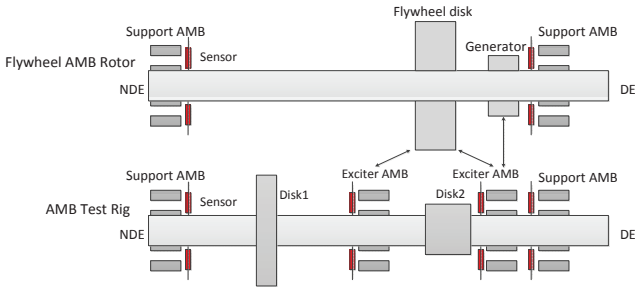

Figure 2: A schematic of the AMB suspended flywheel test tig.

Rotor: The flexible rotor is 1.23 m long and weights 44.9 kg. The rotor is driven by a 3.7 kW motor with a variable frequency drive, Colombo RS-90/2, to speeds up to 18,000 r/min. A custom shaft extension connects the drive to a flexible disk coupling (Rexnord 75CC140140).

AMBs: Four laminated steel journals that are mounted on the rotor for the four radial AMBs. The test rig also contains two auxiliary ball bearings mounted at the locations of the two support AMBs to prevent damage to the AMBs in the event of a rotor drop.

Digital controller: The digital control system is to be implemented on an Innovative Integration M6713 PCI board with a TI C6713B 32-bit floating point DSP chip. The sampling frequency is 12 kHz. Sixteen input-output analog channels that link the 16 sensors to the 16 actuators of the four AMBs are sampled simultaneously.

Amplifier: Each AMB is driven by a Copley Controls PWM amplifier, which operates from a 150V DC power supply with a continuous current rating of 10 A to provide a maximum static load of 1450 N.

Displacement Sensors: The rotor position at the location of each support AMB is measured by a Kaman 1H/15N eddy current probe and an anti-alias filter circuit attenuates the measurement noise. The rotor motion at the location of each exciter AMB is measured by a Bently Nevada 7200 Series eddy current probe, whose output voltage is changed from -10V to 0V by a gain and offset circuit.

B. The Characteristic Model Based ACAC

The basic idea of characteristic modeling is that a higher order system can be represented equivalently as a lower order, often first and second order, time-varying linear system, which, when the sampling period is sufficiently small, has the same output as the original system at the sampling instants. This lower order system is called the characteristic model of the original system [18], [19]. The time-varying coefficients of the characteristic model, referred to as the characteristic parameters, are then identified online adaptively. Based on the characteristic model, a simple PID type control law is designed. The resulting feedback law is referred to as the characteristic model based all-coefficient adaptive control (ACAC) law. A schematic diagram of the characteristic model based ACAC system is depicted in Figure 3.

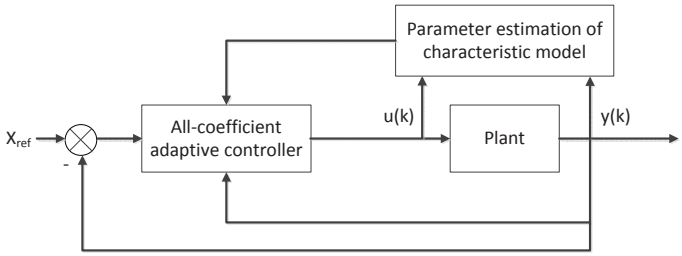

Figure 3: A diagram of the characteristic model based ACAC system.

1) Characteristic modeling: Let a linear time-invariant system be described by the transfer function,

$$G(s) = \frac{b_m s^m + b_{m-1}s^{m-1} + \cdots + b_1 s + b_0}{s^n + a_{n-1}s^{n-1} + \cdots + a_1 s + a_0}, \qquad (2)$$

where a_i's and b_i's are constant parameters of the plant. It has been established in [18], [19] that, if the control objective is position keeping or reference tracking and the sampling period T is sufficiently small, the characteristic model takes the following form,

$$\begin{aligned} y(k) \;=\; & f_1(k)y(k-1) + f_2(k)y(k-2) + g_0(k)u(k-1) \\ & + g_1(k)u(k-2), \end{aligned} \qquad (3)$$

where $u(k)$ is the control input, $y(k)$ is the system output, and $f_1(k)$, $f_2(k)$, $g_0(k)$ and $g_1(k)$ are the characteristic parameters. Despite its simplicity, the characteristic model produces the same output as the original model (2) at each sampling instant. Characteristic modeling is different from the conventional model reduction methods in that it compresses the plant information into the time-varying coefficients instead of truncating parts of the plant model. The characteristic parameters, $f_1(k)$, $f_2(k)$, $g_0(k)$ and $g_1(k)$, are identified by the gradient adaptive law.

2) Characteristic model based ACAC: The characteristic model based ACAC law takes the following form,

$$u_c(k) = u_O(k) + u_G(k) + u_D(k) + u_I(k), \qquad (4)$$

where,

$$\begin{aligned} u_O(k) &: \quad \text{maintaining/tracking control,} \\ u_G(k) &: \quad \text{golden section adaptive control,} \\ u_D(k) &: \quad \text{differential control,} \\ u_I(k) &: \quad \text{integral control,} \end{aligned}$$

and are respectively given by,

$$\begin{aligned} u_O(k) &= \frac{y_r(k) - \hat{f}_1(k)y(k) - \hat{f}_2(k)y(k-1) - \hat{g}_1(k)u_O(k-1)}{\hat{g}_0(k) + \lambda_1}, \\ u_G(k) &= \frac{l_1\hat{f}_1(k)\tilde{y}(k) + l_2\hat{f}_2(k)\tilde{y}(k-1) + \hat{g}_1(k)u_G(k-1)}{\hat{g}_0(k) + \lambda_1}, \\ u_D(k) &= d_1\frac{\tilde{y}(k) - \tilde{y}(k-1)}{T}, \\ u_I(k) &= u_I(k-1) + d_2\tilde{y}(k), \end{aligned}$$

where $y_r(k)$ is the reference output, λ_1 is a positive constant, $\tilde{y}(k) = y_r(k) - y(k)$, $l_1 = 0.382$, $l_2 = 0.618$, d_1 and d_2 are both positive constants.

C. Simulation and Experiment Results

The simulation results of the rotor displacements without and with the generator negative stiffness in [11] shows the effect caused by the generator is minimal and negligible. In the simulation of the rotor orbits with the actual gyroscopic matrix G and with the emulated gyroscopic forces, the similar patterns and the orbits tilting phenomenon indicate the feasibility of the flywheel emulation approach. All the simulation results are verified by the experimental test results. As a result, we provided an experimental flywheel AMB platform to study the the control design for the energy storage flywheels in [11].

Because of the complex dynamics and the presence of strong uncertainties, the flywheel AMB system was first stabilized by the μ-synthesis controller. Then the characteristic model based ACAC designs have been implemented on this flywheel emulation platform to study the control design for flywheels. An identical characteristic model based ACAC law as a substitute for the μ-synthesis controller is implemented for each of the four control channels, the x and y axes of the two support AMBs. Shown in Figure 4 are the simulated rotor orbits under the μ-synthesis controller (black curves) in comparison with the corresponding orbits (red curves) under the characteristic model based ACAC , where the polar moment of inertia of the emulated flywheel is $J_\mathrm{p} = 0.042\,\mathrm{kg{\cdot}m^2}$, the transverse moment of inertia is $J_\mathrm{t} = 0.021\,\mathrm{kg{\cdot}m^2}$ and $\Omega = 7,600\,\mathrm{r/min}$. In the figure, the four plots, dnx-dny, dmx-dmy, dqx-dqy and ddx-ddy, are respective the orbits at the locations of the non-driven end bearing, mid span bearing, quarter span bearing and the driven end bearing. It is observed that the displacements in both x and y axes at the locations of the two support AMBs are much smaller under the characteristic model based ACAC.

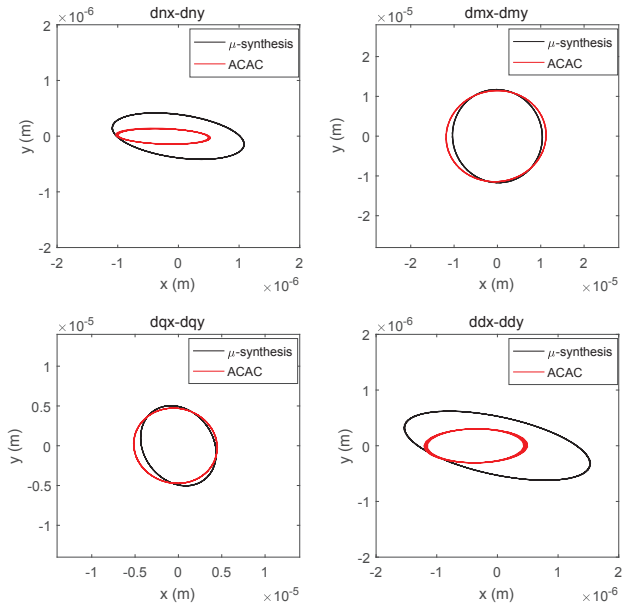

Figure 4: Simulation results of the orbits at $\Omega = 7,600\,\mathrm{r/min}$: μ-synthesis controller vs characteristic model based ACAC.

Figure 5 shows the experimental rotor orbit comparison under two controllers with $J_\mathrm{p} = 0.021\,\mathrm{kg{\cdot}m^2}$ and $\Omega = 7,600\,\mathrm{r/min}$. The blue curves are the experimental results under the μ-synthesis controller and the red curves are the rotor orbits under the characteristic model based ACAC law. We can observe that the characteristic model based ACAC design results in smaller rotor orbits at all AMB locations, which represent approximately a 50% reduction in vibration at the location of the NDE AMB location, a 60% reduction at the locations of the two exciter AMBs, and a 25% reduction at the location of the DE AMB location. To sum up, the simulation and experiment results all validate that the characteristic model based ACAC can achieve a better effect in vibration suppression of the AMB suspended energy storage flywheel test rig than the μ-synthesis controller could.

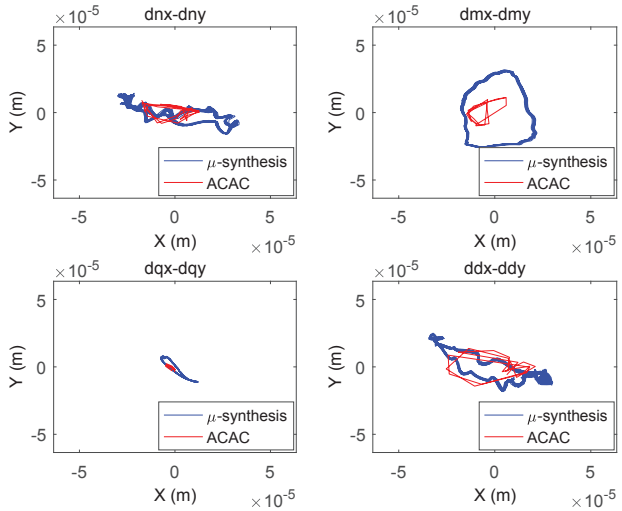

Figure 5: Experimental rotor orbits at $\Omega = 7,600\,\mathrm{r/min}$: μ-synthesis controller vs characteristic model based ACAC.

III. Performance of the Characteristic Model Based ACAC in the Presence of Time Delays

The inevitable time delay phenomenon in the closed control loop could affect the performance and the stable operation of the flywheel AMB system. Based on the simulation and experimental results of the characteristic model based ACAC we have implemented on the AMB suspended energy storage flywheel platform, the performance of the test rig in the presence of control input delay, sensor output delay and both under the characteristic model based ACAC design is investigated.

The Simulink model is based on the state space form with 36 states, 12 inputs and 20 outputs [11]. The currents generated by the exciter AMBs are calculated based on the polar moment of inertia and transverse moment of inertia of the emulated flywheel, which are $J_\mathrm{p} = 0.042\,\mathrm{kg{\cdot}m^2}$ and $J_\mathrm{t} = 0.021\,\mathrm{kg{\cdot}m^2}$ respectively. The rotating speed is $\Omega = 7,600\,\mathrm{r/min}$. The initial values for the estimation of the characteristic model are selected as $f_1(0) = 2.102$, $f_2(0) = -1.104$ and $g_0(0) = g_1(0) = 0.001$, and the parameters in the adaptation law are chosen as $\delta = 3.5$ and $\gamma = 1.5$ in all channels. The control

parameters in all control channels are $\lambda_1 = 0.2$, $d_1 = 0.02$ and $d_2 = 10$.

A. In the Presence of Control Input Delay

The input delay is introduced in the simulation. The length of the time delay τ is usually a multiple of the sample time $T_s = 8.33 \times 10^{-5} s$ of the digital controller.

The rotor orbit of the flywheel AMB test rig under the characteristic model based ACAC with control input delay $\tau = T_s$ is shown in Figure 6. Compared to the orbit (in red curve) in Figure 4, it is observed that this control design possesses the ability to resist the effect of the time delay $\tau = T_s$ on the control input.

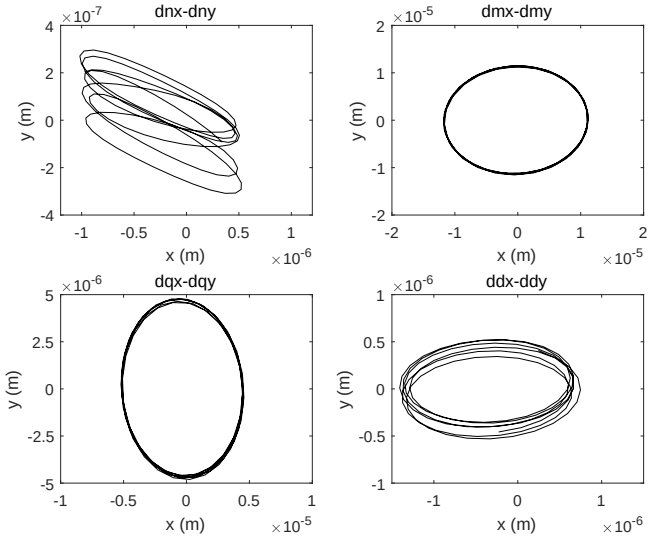

Figure 6: Simulation results of the orbits under the characteristic model based ACAC at $\Omega = 7,600$ r/min with control input delay $\tau = T_s$.

Then we set the input delay to two times the sampling time of the digital controller. Figure 7 shows the flywheel rotor orbit under the characteristic model based ACAC with control input delay $\tau = 2T_s$. This controller resists the impact of input delays once again. Compared to the flywheel rotor orbit under the characteristic model based ACAC with control input delay $\tau = 2T_s$ in Figure 6, the shape of the orbit in Figure 7 changes slightly at the NDE AMB and DE AMB. The maximum amplitude of displacements in both x and y axes at the locations of the four AMBs in these two cases are all smaller than 2×10^{-5} m.

B. In the Presence of Sensor Output Delay

We next consider the effect of the sensor output delay. We first set the sensor output delay to one time the sampling time of the digital controller in Figure 8, then two times in Figure 9. It is observed from the flywheel orbits in Figure 8 and Figure 9 that the flywheel AMB system remains stable under the characteristic model based ACAC with sensor output delay $\tau = T_s$ and $\tau = 2T_s$.

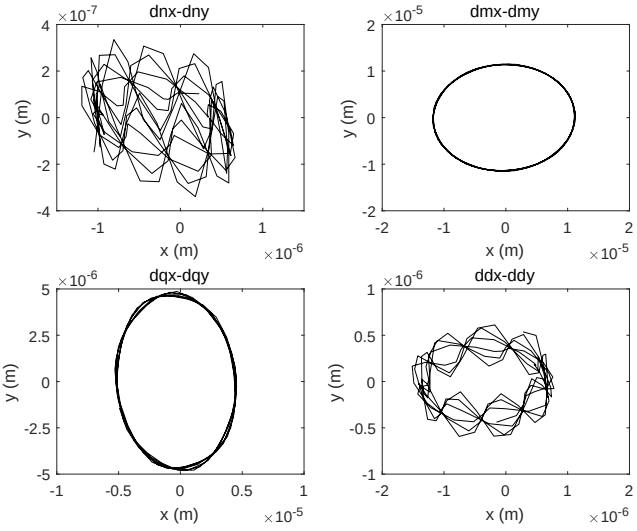

Figure 7: Simulation results of the orbits under the characteristic model based ACAC at $\Omega = 7,600$ r/min with control input delay $\tau = 2T_s$.

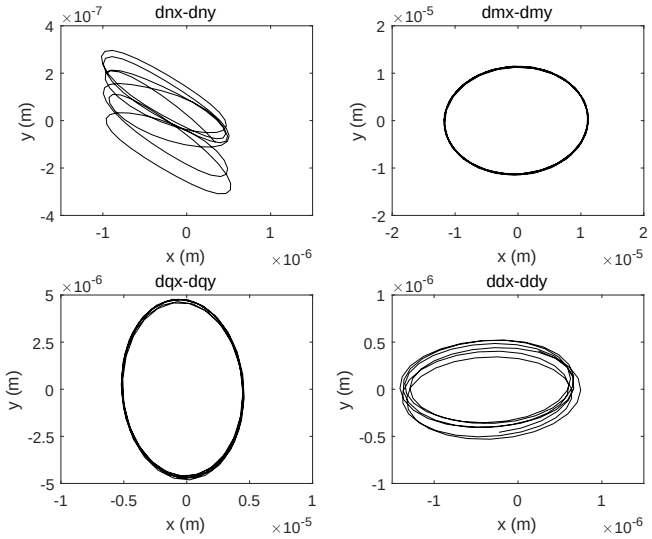

Figure 8: Simulation results of the orbits under the characteristic model based ACAC at $\Omega = 7,600$ r/min with sensor output delay $\tau = T_s$.

C. In the Presence of Control Input Delay and Sensor Output Delay

We now consider the simulation when both the control input delay and sensor output delay are present. Figure 10 shows the flywheel rotor orbits under the characteristic model based ACAC with the control input delay $\tau = T_s$ and sensor output delay $\tau = T_s$. The controller is capable of resisting the influence of two types of time delays.

IV. Conclusions

The performance of the characteristic model based ACAC on AMB suspended energy storage flywheel test rig in the presence of time delays was investigated in this paper. First

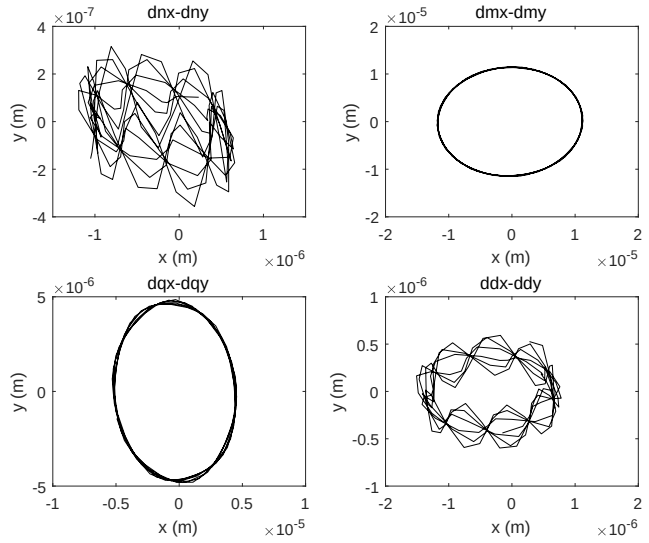

Figure 9: Simulation results of the orbits under the characteristic model based ACAC at $\Omega = 7,600$ r/min with sensor output delay $\tau = 2T_s$.

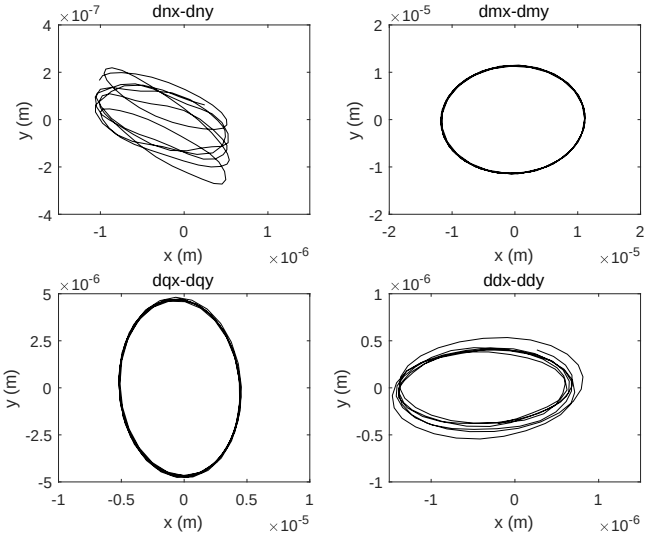

Figure 10: Simulation results of the orbits under the characteristic model based ACAC at $\Omega = 7,600$ r/min with control input delay $\tau = T_s$ and sensor output delay $\tau = T_s$.

the experimental platform for AMB suspended energy storage flywheel which was developed on the basis of a flexible rotor-AMB test rig previously constructed in the ROMAC Laboratory, University of Virginia was reviewed. Next, the rotor behavior of the flywheel emulation platform under the characteristic model based ACAC was briefly presented. The performance of the closed-loop flywheel AMB system in the presence of control input delay and sensor output delay under the characteristic model based ACAC was tested in the simulation. The simulation results of rotor orbits in the presence of the input delays $\tau = T_s$ and $\tau = 2T_s$, sensor output delays $\tau = T_s$ and $\tau = 2T_s$, and both input and sensor output delays $\tau = T_s$ indicate that the characteristic model based ACAC possesses considerable ability to resist the adverse effect of time delays on the AMB suspended energy storage flywheel test rig.

REFERENCES

[1] H. Zhao, Q. Wu, S. Hu, H. Xu and C. N. Rasmussen, "Review of energy storage system for wind power integration support," *Applied Energy*, vol. 137, pp. 545-553, 2015.

[2] S. Koohi-Kamali, V. V. Tyagi, N. A. Rahim, N. L. Panwar and H. Mokhlis, "Emergence of energy storage technologies as the solution for reliable operation of smart power systems: A review," *Renewable and Sustainable Energy Reviews*, vol. 25, pp. 135-165, 2013.

[3] F. Faraji, A. Majazi, and K. Al-Haddad, "A comprehensive review of flywheel energy storage system technology," *Renew Sust Energ Rev*, vol. 67, pp. 477-490, 2017.

[4] R. Hebner, J. Beno, and A. Walls, "Flywheel batteries come around again," *IEEE Spectr*, vol. 39, pp. 46-51, 2002.

[5] C. M. Reid, T. B. Miller, M. A. Hoberecht, P. L. Loyselle, L. M. Taylor, S. C. Farmer, and R. H. Jansen, "History of electrochemical and energy storage technology development at NASA Glenn Research Center," *J Aerosp Eng*, vol. 26, pp. 361-371, 2013.

[6] M. Farhadi, and O. Mohammed, "Energy storage technologies for high-power applications," *IEEE Trans Ind Appl*, vol. 52, pp. 1953-1961, 2016.

[7] H. Zhao, Q. Wua, S. Hu, H. Xu, and C. N. Rasmussen, "Review of energy storage system for wind power integration support," *Appl Energy*, vol. 137, pp. 545-553, 2015.

[8] G. Schweitzer and E. H. Maslen, *Magnetic Bearings: Theory, Design, and Application to Rotating Machinery*, Berlin: Springer, 2009.

[9] G. Li, Z. Lin, P. E. Allaire and J. Luo, "Modeling of a high speed rotor test rig with active magnetic bearings," *Journal of Vibration and Acoustics*, vol. 128, no. 3, pp. 269-281, 2006.

[10] R. Arghandeh, M. Pipattanasomporn and S. Rahman, "Flywheel energy storage systems for ride-through applications in a facility microgrid," *IEEE Trans Smart Grid*, vol. 3, pp. 1955-1962, 2012.

[11] X. Lyu, L. Di, S. Y. Yoon, Z. Lin and Y. Hu, "A platform for analysis and control design: Emulation of energy storage flywheels on a rotor-AMB test rig," *Mechatronics*, vol. 33, pp. 146-160, 2016.

[12] T. P. Dever, G. V. Brown, K. P. Duffy, and R. H. Jansen, "Modeling and development of a magnetic bearing controller for a high speed flywheel system, in *Proceedings of the 2nd International Energy Conversion Engineering Conference*, Providence, RI, 2004. pp. AIAA-2004-5626.

[13] G. V. Brown, A. F. Kascak, R. H. Jansen, T. P. Dever and K. P. Duffy, "Stabilizing gyroscopic modes in magnetic-bearing-supported flywheels by using cross-axis proportional gains, in *Proceedings of the AIAA Guidance, Navigation, and Control Conference*, San Francisco, California, 2005. pp. AIAA-2005-5955.

[14] C. Peng, Y. Fan, Z. Huang, B. Han and J. Fang, "Frequency-varying synchronous micro-vibration suppression for a MSFW with application of small-gain theorem," *Mech Syst Signal Proc*, vol. 82, pp. 432-447, 2017.

[15] S. Sivrioglu, K. Nonami and M. Saigo, "Low power consumption nonlinear control with H_∞ compensator for a zero-bias flywheel AMB system," *J Vib Control*, vol. 10, pp. 1151-1166, 2004.

[16] S. E. Mushi, Z. Lin and P. E. Allaire, "Design, construction, and modeling of a flexible rotor active magnetic bearing test rig," *IEEE/ASME transactions on mechatronics*, vol. 17, no. 6, pp. 1170-1182, 2012.

[17] L. Di and Z. Lin, "Control of a flexible rotor active magnetic bearing test rig: a characteristic model based all-coefficient adaptive control approach," *Control Theory Technol*, vol. 12, pp. 1-12, 2014.

[18] H. Wu, J. Hu and Y. Xie, "Characteristic model-based all-coefficient adaptive control method and its applications," *IEEE Trans Syst Man Cybern Part C-Appl Rev*, vol. 37, pp. 213-221, 2007.

[19] H. Wu, J. Hu, and Y. Xie, *Characteristic Model-based Intelligent Adaptive control (in Chinese)*, Beijing: China Science and Technology Press, 2009.

[20] X. Lyu, L. Di, Z. Lin, Y. Hu and H. Wu, "Characteristic model based all-coefficient adaptive control of an AMB suspended energy storage flywheel test rig," *SCIENCE CHINA Information Sciences*, 2018, doi:10.1007/s11432-017-9327-0.

[21] J. P. Richard, "Time-delay systems: an overview of some recent advances and open problems," *Automatica*, vol. 39, no. 10, pp. 1667-1694, 2003.

[22] Y. Ren, X. Chen, Y. Cai and W. Wang, "Rotation modes stability analysis and phase compensation for magnetically suspended flywheel systems with cross feedback controller and time delay," *Mathematical Problems in Engineering*, 2016, doi: 10.1155/2016/3783740.

[23] A. F. Kascak, G. V. Brown, R. H. Jansen and T. P. Dever, “Stability limits of a PD controller for a flywheel supported on rigid rotor and magnetic Bbearings,” in *Proceedings of the AIAA Guidance, Navigation, and Control Conference*, San Francisco, California, 2005. pp. AIAA-2005-5956.

[24] S. Y. Yoon, L. Di, P. Anantachaisilp and Z. Lin, “Truncated predictor feedback control for active magnetic bearing systems with input delay,” *IEEE Transaction on Control Systems Technology*, vol. 24, no. 6, pp. 2182-2189, 2016.